Towards reproducible measurement of nanoparticle size using dynamic light scattering: Important controls and considerations

Dominique Langevin, Eric Raspaud, Sandrine Mariot, A. Knyazev, A. Stocco, Anniina Salonen, A. Luch, A. Haase, B. Trouiller, C. Relier, et al.

On the measurement of nanoparticle size using Dynamic Light Scattering. Advantages and drawbacks of commercial instruments

D.Langevin[1], E.Raspaud[1], S.Mariot[1], A.Knyazev[1*], A.Stocco[1**], A.Salonen[1], A. Luch[2], A.Haase[2], B. Trouiller[3], C. Relier[3], O. Lozano[4§], S.Thomas[5], A.Salvati[5$], K.Dawson[5].

1. Laboratoire de Physique des Solides, CNRS, Univ. Paris Sud 11, Université Paris Saclay, 91405 Orsay, France
2. German Federal Institute for Risk Assessment, Department of Chemical and Product Safety, 10589 Berlin, Germany
3. Namur Nanosafety Centre (NNC), Namur Research Institute for LIfe Sciences (NARILIS), Research Centre for the Physics of Matter and Radiation (PMR), University of Namur, Namur, Belgium.
4. Ineris, Parc Technologique Alata, BP2, 60550 Verneuil en Halatte, France

* present address: Baxalta Manufacturing, Route Pierre-à-Bot 111 2000 Neuchâtel, Switzerland

** present address: Laboratoire Charles Coulomb, CNRS, Université Montpellier 2, Montpellier, France

§ present address : Centro de Investigación Básica y Transferencia, Hospital Zambrano-Hellion. Tec Salud. Tecnológico de Monterrey, Mexico.

$ present address : Groningen Research Institute of Pharmacy, University of Groningen, 9713AV Groningen, the Netherlands

Abstract

It is prerequisite to characterize nanoparticles in dispersions in particular with respect to their size and size distribution before they can be used in toxicological testing. This requires robust methods with high reproducibility. The aim of this study was to apply interlaboratory comparisons using Dynamic Light Scattering (DLS), in order to evaluate the reproducibility of nanoparticle size determinations. DLS is well established in most nanotoxicological laboratories. Due to the fact that this technique appears easy to use it has become a standard technique nowadays. Still, reproducibility and in particular differences between different commercial instruments have not been addressed systematically before. Our aim was to develop a robust standard operating procedure (SOP). Therefore, at the beginning, experiments were performed with dispersions of rather monodisperse and spherical particles in water. Significant differences were observed between the results obtained with different commercial instruments for DLS, especially when fitting the data using mathematical inversion methods. As a consequence of the different settings applied when fitting the data, significant errors could be made especially when working with dilute dispersions of very small particles. Here we have identified options how to overcome possible issues.

However, It should be noted, that in practice, nanoparticles may have significant polydispersities and/or be non-spherical. The potential of the DLS technique in this situation should be noted that in nanoparticles may have significant polydispersities and/or be non-spherical. The potential of the DLS technique in this situation is evaluated. A combination of two different techniques (DLS and electron microscopy for instance) is recommended to fully interpret the results.

1. Introduction

Light scattering (1) is a well-known phenomenon, responsible in particular for the blue color of sky: light from the sun is scattered by particles in the atmosphere, the scattering being more important for the smaller wavelengths, hence the blue component of the sun light spectrum dominates the scattering. Particles in the atmosphere are very dilute, so there are no interferences between the light scattered by the different particles. In liquid dispersions of nanoparticles, the interparticle distance is in general smaller than the wavelength of light, so the scattering should in principle disappear. The scattered intensity (per particle) indeed becomes very small, but does not vanish. This is due to the Brownian motion of the nanoparticles: the dispersion is not fully homogeneous, some regions contain more particles than others at a given time. As a result of this motion, a spectral broadening due to Doppler effect occurs, of order D/λ^2, D being the particle diffusion coefficient and λ the light wavelength. For nanoparticles of 20 nm radius in water and a wavelength of 600 nm, the broadening is of the order of 1000 Hz. In order to detect such a small broadening, laser sources should be used. By measuring the broadening of laser spectral lines, or alternatively the time correlation function of the scattered intensity, the diffusion coefficient D can be determined. Knowing D, the particle size can be obtained. This method is called Dynamic Light Scattering (DLS)(2). DLS was developed in the 1960s and 70s, after lasers became available. Today, many commercial instruments can be purchased. Among the very popular ones, several benchtop instruments determine not only the zeta potential of the particles, but also their size, as they make use of light scattering for both determinations. Such instruments nowadays are extensively used in standard characterization laboratories because they are simple to operate and not too expensive. However, the measurements are automatized to a large extent, which can produce errors in size determinations. When the particles have a rather well defined size and when they are spherical, these instruments provide reliable results provided the data analysis is performed with care. When the particles are very polydisperse and/or when they have non-spherical shapes, more sophisticated instruments are necessary. It should be noted that the intensity of the light scattered by particles increases as the sixth power of the diameter, so the signal is dominated by the largest particles. When the dispersions contain both large and small particles, the small ones can hardly be detected.

The present paper describes the problems that can arise and proposes solutions to avoid them.

2. Principle of the method

Figure 1 shows a scheme of the method. A light source illuminates the sample and the scattered light is detected at a scattering angle θ.

We will briefly recall below the principle of DLS data analysis. Useful supplementary information and practical details can be found for instance in ref (3).

The DLS instruments measure in general the correlation function of the scattered intensity I :

$$g_2(\tau) = \langle I(t)\, I(t+\tau)\rangle / \langle I(t)^2\rangle$$

which is the Fourier transform of the power spectrum of the scattered light; t is time and τ is the lag time.

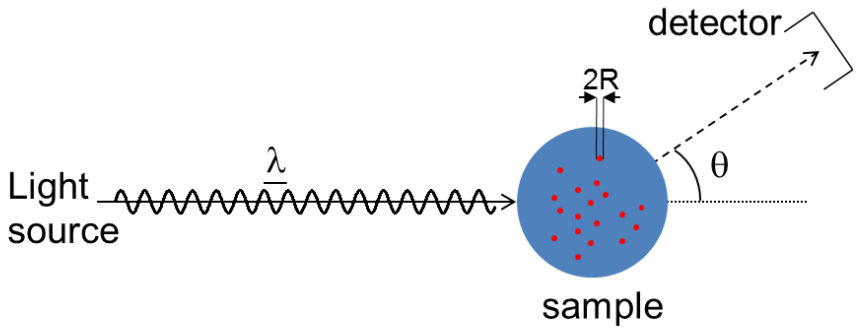

Figure 1. Scheme of the DLS procedure

In the ergodic limit (space and time averages identical), this correlation function is related the correlation function for the scattered electric field E,

$$g_1(\tau) = \langle E(t)\, E(t+\tau)\rangle / \langle E(t)^2\rangle$$

through the Sigert relation:

$$g_2(\tau) = 1 + \beta g_1(\tau)^2$$

where β is an instrumental parameter ($0<\beta<1$). When the particles are monodisperse:

$$g_2(\tau) = 1 + \exp(-\tau/\tau_D) \qquad (1)$$

with

$$\tau_D = 1/(2Dq^2) \qquad (2)$$

D being the diffusion coefficient and q the wave vector: $q = 4\pi n \sin(\theta/2)/\lambda$, with n the solution refractive index and λ the wavelength of light. If the dispersions are dilute so that interactions between particles can be neglected, D is given by the Stokes-Einstein formula:

$$D_{st} = \frac{k_B T}{6\pi\eta R_h} \qquad (3)$$

k_B being the Boltzmann constant, T the absolute temperature, η the viscosity of the liquid used to disperse the particles and R_h their hydrodynamic radius.

In the best commercial instruments, a goniometer allows to systematically vary the scattering angle θ, hence the wave vector q. The validity of equation 2 can then be checked, proving that the particle motion is Brownian, and very precise values of the diffusion coefficient and particle size are obtained. In other commercial instruments, the detector is fixed, usually in backscattering conditions ($\theta \sim 170°$). The influence of eventual convection in the sample cannot be evaluated and the accuracy on the particle size is lower.

When the dispersions are not dilute, interactions between particles start playing a role and D differs from the Stokes expression: D is larger for repulsive particles, smaller for attractive ones. For dispersions containing a few percent particles in volume:

$$D \sim D_{st} (1 + \alpha \phi) \quad (4)$$

ϕ being the particle volume fraction. In the special case of hard-sphere interactions α ~1.5 (4). In general α is of order of unity, so little error is made calculating the particle radius with the Stokes formulas provided the volume fraction is less or close to about 1%.

In practice, particles are never monodisperse, and the correlation function is a superposition of functions corresponding to the different particle sizes. When the polydispersity is not too high, the correlation function can be written as a *cumulant* expansion:

$$ln[g_2(\tau) - 1] \cong -\frac{\tau}{\tau_D} + \frac{\mu_2}{2}\left(\frac{\tau}{\tau_D}\right)^2 \quad (5)$$

where $\mu_2/2$ is the polydispersity index (PDI). In the case of a Gaussian distribution of sizes around a mean size $\bar{R}$:

$$f(R) = \frac{1}{\sigma\sqrt{2\pi}}\, e^{-\frac{(R-\bar{R})^2}{2\sigma^2}} \quad (6)$$

the PDI is equal to σ.

In the cumulant method, the mean radius $\bar{R}_{cum}$ is calculated from the characteristic time τ_D in equation 5 using equations 2 and 3. $\bar{R}_{cum}$ is therefore a harmonic average (usually called Z-average). For an extremely narrow monomodal distribution, $\bar{R}_{cum}$ should be equal to the average radius from the size distribution $\bar{R}$, but with even a small poly-dispersity $\bar{R}_{cum}$ is smaller than $\bar{R}$. In general, the cumulant method is considered useful only if the distribution is relatively monodisperse (i.e. PDI $\lesssim$ 0.5).

When the polydispersity is larger, other types of analysis are required. The correlation function $g_1(\tau)$ is, as explained above, the sum of exponentials corresponding to the different sizes of the particles present in the dispersion. The size distribution can therefore in principle be obtained by taking the Laplace transform of this correlation function. Unfortunately, and at the difference of the Fourier Transform, a Laplace transform is very sensitive to noise and fast and efficient algorithms do not exist. Some commercial instruments allow using an inversion method named CONTIN. This well-documented computation routine utilizes regularized non-negative least-squares techniques combined with eigenfunction analysis. As there is no unique answer to the inversion problem, CONTIN choses the least detailed distribution consistent with the data. It assumes in particular that sharp peaks are improbable, so the analysis will in general broaden the distribution for extremely monodisperse particles. In addition, because of the noise problem, the quality of the correlation function data needs to be excellent in order to retrieve the actual size distribution. When this is the case, it has been shown that even complex multimodal distributions can be retrieved (5). The different commercial instruments use their own improved inversion routines and since the algorithms are proprietary, little information about the exact type of algorithm is available.

Although it is usually recommended to measure the correlation function up to 10^4 times τ_D in order to be able to analyse the data with sophisticated routines such as CONTIN, it is essential to discard the data for times much longer than τ_D if a cumulant analysis is performed.

3. Spherical particles with small polydispersity

We will discuss examples of measurements done with polystyrene particles coated by amine groups, called afterwards PS-NH_2 particles. These particles were obtained from a commercial source of nominally 50 nm PS-NH_2 nanoparticles as an aqueous dispersion (Bangs Laboratories PA02 N-8626) and were used for a small Round Robin test between three different laboratories. The starting dispersion was diluted to a concentration of 1 mg/ml in MilliQ grade water and aliquots of the same dispersion were distributed to the 3 participating laboratories (UCD, Ireland; UPS, France and BfR, Germany). For the measurement, the particle dispersions were further diluted in pure water by a factor ten in each laboratory to reach a final concentration of 100 µg/ml. The sample preparation and the measurement were performed following a standard operating procedure (SOP) established within the EU funded Research Infrastructure QualityNano (6)

The measurements have been done using three different commercial DLS instruments (from different manufacturers, the scattering angle being the same, 173°, and the sources being either LEDS or lasers with $\lambda\sim$ 650 nm. The corresponding results are given using numbers 1-3 for the different instruments. Experiments were also performed in a home-made instrument in UPS (7). The temperature was set at 25°C. We show typical results in Figure 2.

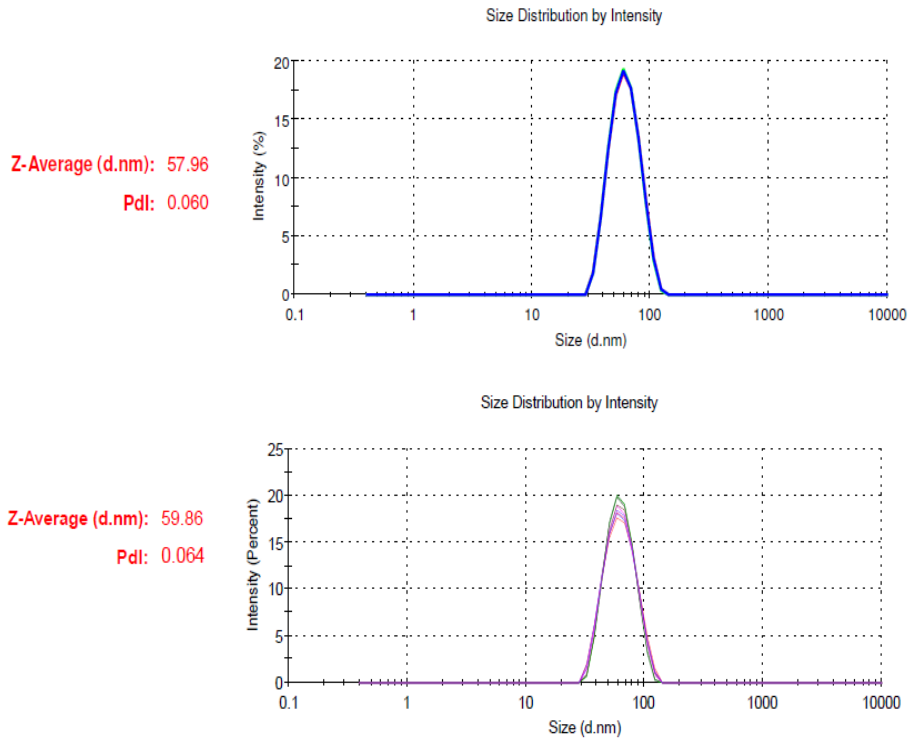

Figure 2. Diameter distributions of PS-NH2 particles obtained by instruments 1 and 2. The Z-average diameter comes from the cumulant analysis while the distribution plotted comes from a Contin analysis

The experiments done with the home-made instrument and the same sample were fully consistent with those of Figure 2, diameter 58 nm, PDI<10%. A simple exponential fit of the correlation function was performed in this last case, as it is known that PDI values less than 10% can hardly be measured using DLS. The results are shown in table 1.

The commercial instruments allow not only an analysis by the cumulant method, but also by inversion methods such as CONTIN. When using the inversion methods, the results are different, the diameter and the PDI are larger (see table 1). Reason for this difference were already discussed in §2.

Laboratory	Diameter,nm (cumulants)	PDI (cumulants)	Diameter,nm (inversion method)	PDI (inversion method)
Zetasizer 1	58	0.06	61.2	0.16
Zetasizer 2	60	0.06	62.4	0.06
Zetasiser 3	65	0.23	95	0.75
home made instrument	58	< 0.1		

Table 1. Measured sizes and polydispersity of the PS-NH2 nanoparticles from the different instruments and using different analysis procedures. The numbers are averages of experiments made three times, each with three different samples.

The results obtained with the benchtop instrument 3 are compatible, although slightly larger. The cumulant analysis leads to a mean diameter of 65 nm and a significantly larger PDI: 0.23. Figure 3 shows the size distributions obtained with the inversion method: as for the other instruments, 3 different cells were used and 3 correlation functions measured for each cell. The PDI significantly varies from one curve to another, from 0.07 to 0.50. This is accompanied by a large variation of the average diameter, between 61 and 76 nm.

In order to search for the possible origin of these discrepancies, we have looked in more detail at the correlation function $g_2(\tau)$ obtained with the instrument 3 for one of the 9 experiments that led to a diameter of 61.2 nm and a PDI of 0.123. The correlation function $g_2(\tau)$ was measured for τ between 0 and 1 second, although the main decrease occurs during the first millisecond. It is therefore possible that the noise introduced by non-significant long time data produces artefacts in the fitting procedure.

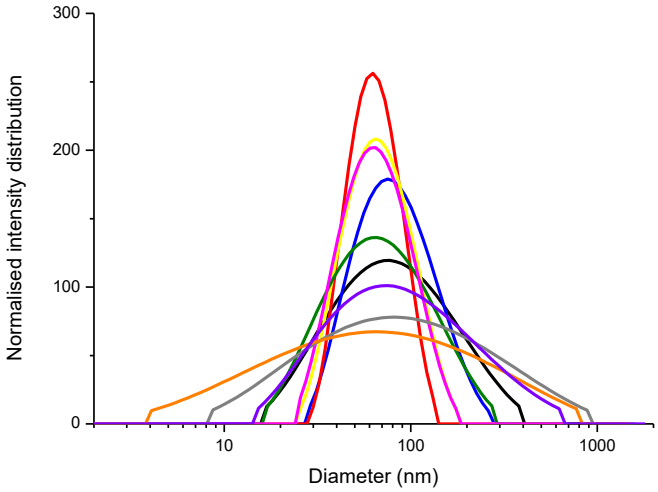

Figure 3. Size distribution (intensity averaged) of a dispersion of PS-NH2 particles obtained from the instrument 3. The curves correspond to samples prepared by dilution of a unique sample to the same final concentration (three different samples), or to different aliquots of the same solution. The PDI indicated in table 2 corresponds to the average of the 9 distributions.

We have therefore kept only the data between 1 and 400 μs (Figure 4). Above 400 μs, $g_2(\tau)$ is equal to 1 within less than 10^{-2} and some values of g_2-1 are negative; in this case, ln (g_2-1) is not defined and no fit can be performed. The instrument's software suppresses data points, but one has to specify a minimum value for g_2, the recommended value from the manufacturer being 1.003. Note that in our fits, we have cut all the points above τ = 400μs, and g_2 was always larger than 1. In the data used by the instrument, g_2 values of 1.003 are found already for times as short as 3800 μs.

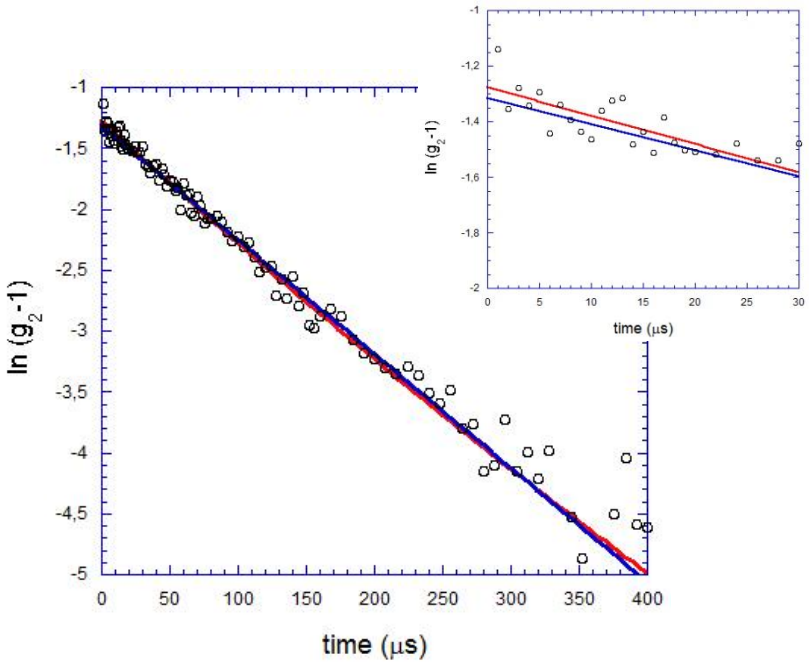

Figure 4. Correlation function measured for lag times τ up to 400μs. Linear(blue line) and cumulant fits (red line). Inset: Correlation function at shorter times, up to 30μs.

Two fits were performed for ln [$g_2(\tau)$-1], a linear fit and a polynomial (cumulant) fit using equations 1 and 5. They are shown in Figure 4. One sees that the linear fit and the polynomial fit are undistinguishable from one another. This is better seen in Figure 5, restricted to short times, 1-30µs. One also sees that the noise in the data prevents a safe determination of the PDI. In the case discussed, the PDI obtained from the cumulant fit is 0.025, much lower than the value given by the instrument with the same cumulant analysis. The correlation time from this fit leads to a diameter of 60 nm, somewhat smaller than the value given by the instrument, but consistent with those obtained with the other instruments (table 1). This is likely due to the fact that method used by the instrument to remove data points is different from ours. When $g_2 < 1.0003$, the instrument replaces the actual value of g_2 by 1.0003, introducing therefore many large values of g_2 which artificially increase the correlation time and, as a consequence, the particle diameter.

This discussion demonstrates that a poor signal to noise ratio introduces important uncertainties in the determination of the correlation time distribution. It confirms that the cumulant method cannot be safely used without cutting data at times much longer than τ_D. The noise introduces errors in the size distribution and as a consequence, errors in the measured sizes. The problem arises with all instruments when the samples are diluted too much.

The commercial DLS instruments also provide the size distribution by number and by intensity when an inversion analysis is performed. As we have mentioned earlier, these distributions should be handled with caution as the size averages and the polydispersity increase when the noise level increases. . Figure 5 gives an example with the rather monodisperse PS-NH2 particles (PDI 6%) where the intensity averaged diameter is 58 nm, while the number average is only 45 nm.

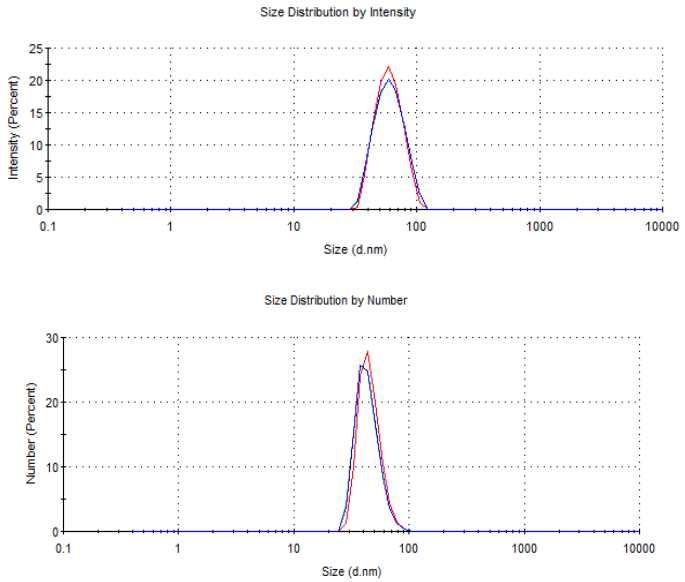

Figure 5. Size distribution by intensity and by number of a dispersion of PS-NH2 particles obtained from the Zetasizer 2.

Since the inversion procedure leads to a size distribution, it is indeed easy to obtain a new distribution, such as number average. This can allow for instance comparisons with size determination made using electron microscopy. As the intensity is proportional to the square of the

particle volume, intensity averages are shifted to large diameter values with respect to number averages as seen in Figure 5.

4. Recommendations to minimize errors

If dilute solutions of small particles are to be investigated, care has to be taken to obtain correct results.

- Some instruments offer the possibility of using different analysis methods (cumulant, Contin). One test could be to check if the different methods are in agreement. We have seen that in the example chosen, this was not the case for the different commercial instruments. In this case, it is better to use the values given by the cumulant method which are the less sensitive to noise level. It should be kept in mind however that the values provided by the cumulant method are smaller than those obtained from the (exact) size distribution.
- In the case of a cumulant analysis, and in order to limit the possible influence of the noise in the data treatment, the range of correlation times investigated should be limited, typically to times above which the correlation function has decreased by a factor of 100. Setting a lower limit for g_2 and using a larger range of correlation times introduces errors.
- An important number is the minimum detected intensity below which the measurements are not reliable. The commercial instruments indicate when the intensity is too low, and the difficulty can sometimes be overcome by removing attenuators. When this is not possible, one can in principle acquire the signal for a longer time. It is our experience that when this occurs, the signal does not significantly improve even after long averaging.
- Some instruments are not very strict with the corresponding noise level. In case of doubt, the intensity can be changed by changing for instance the optical filters or the size of the detection pinhole. If the intensity range is appropriate, the sizes measured should not change.

Other sources of error could be:

- Some instruments adapt automatically the position of the cell. It is important to verify that the light beam does not travel across the meniscus if the liquid volume in the cell is too small.
- In general, glass cells or plastic cells are provided with the instruments. If the particles adsorb on glass or plastic, the results will not be reliable.

5. Very polydisperse and/or non spherical particles

5.1 Large polydispersity

The intensity of the light scattered by particles increases as the power 6 of the diameter, so the signal is dominated in general by the largest particles. When the dispersions contain both large and small particles, the small ones can hardly be detected.

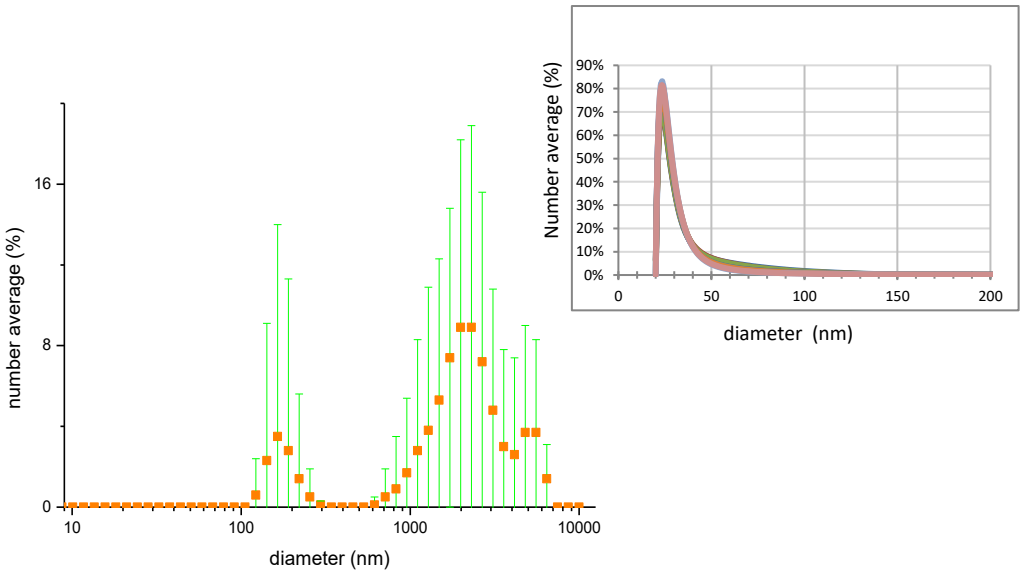

Figure 6. Number distribution of TiO_2 particles dispersed in a phosphate buffer as deduced from Contin analysis of DLS data from a Zetasizer. Inset : distribution obtained with the DCS technique with the same samples.

An example is given in Figure 6 with titanium oxide nanoparticles dispersed in a phosphate buffer. The TiO_2 nanoparticles used were purchased from Evonik (AEROXIDE® TiO_2 P25). The diameter of these particles is 21 nm. They were first dispersed by sonication in ultrapure water, at 21°C. The final solutions, at 0.63, 3.17 and 12.67 mg/ml were prepared in phosphate buffered saline (PBS 10X, Gibco #7011-036). The ionic strength of the buffer is large (around 0.1 M), which leads to partial aggregation of the particles. Whatever their concentration, large aggregates were detected. A number distribution, averaged over 9 measurements is shown in Figure 6.

The instrument indicated that the results do not meet quality criteria: the polydispersity is too high for distribution analysis and even for cumulant analysis. Interestingly, experiments were performed on the same samples using a different method, differential centrifugal sedimentation (DCS) (8; 9) and the distribution obtained was centered on the nominal size of 21 nm. DCS is a technique based on the use of centrifugal force on a spinning disk to fractionate samples by size and density, performing the measurements with a laser source almost at the end of the disk. For a sample with multiple populations of the same material (hence the same density), the sample will be fractionated by populations, ensuring the hydrodynamic measurement of each population individually. This result confirms that the original small particles are still present and that the amount of aggregates is much less than suggested by Figure 6, even when calculated number distributions are plotted.

This example illustrates the limitations of DLS measurements at a single scattering angle, clearly not appropriate to characterize partially aggregated particles.

5.2 Non-spherical particles

Commercial light scattering instruments equipped with goniometers in order to vary the scattering angle are able to determine not only the mean particle size, but also the shape when the particles are large enough (R > 10 nm). These instruments use a combination of the gyration radius R_g, determined from the angular variation of the static scattered intensity, and of the hydrodynamic

radius R_h, determined from classical DLS. R_g can be calculated plotting the static scattered intensity I as a function of q^2, $I(q) \approx 1-(q R_g)^2/3$ for $qR_g \ll 1$ and for dilute particle concentrations (2).

If we take the example of rods of length L and circular section of radius r with large aspect ratio (10) :

$$R_g = \left(\frac{L^2}{12} + \frac{r^2}{2}\right)^{1/2} \quad (7)$$

$$R_h = \frac{L}{2\, ln\left(\frac{L}{2r}\right)} \quad (8)$$

R_g and R_h depend on L and r in different ways, hence their measurement allow the determination of both L and r.

Another method makes use only of the intensity correlation function and is applicable to all nanoparticles. We will give an example below. When particles are not spherical, their rotation also gives rise to light scattering and to a spectral broadening related to the rotation diffusion coefficient D_{rot}. Analysing the correlation functions for polarized and depolarized scattering allows the determination of both D_{rot} and the translation diffusion coefficient D. Again for rod-like particles (10):

$$D = \frac{k_B T}{3\pi\eta L} \ln \frac{L}{2r}$$

$$D_{rot} = \frac{3k_B T}{\pi\eta L^3} \ln \frac{L}{4r} \quad (9)$$

Other expressions were proposed (11), but they do not differ much at large aspect ratio. The method was used for nanotubes by Shetty et al (12), we will give an example here. We measured the polarized (VV) depolarized (VH) dynamic light scattering using the homemade light scattering setup of UPS, on which two Glan-Taylor polarizing prisms (CVI Melles Griot, France) were mounted. The nanotubes used were functionalized by the method of (13) in order to disperse them in water.

The polarized and depolarized electric field correlation functions $g_{VV}(q,t)$ and $g_{VH}(q,t)$ are shown in Figure 7. We fitted these autocorrelation functions with an exponential decay and a first order cumulant term (equation 5).

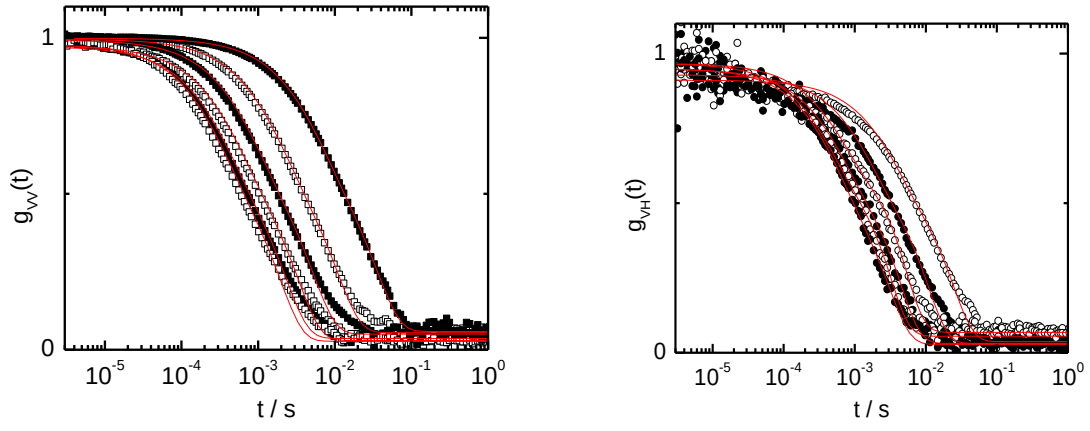

Figure 7. Correlation functions g_{VV} and g_{VH} at scattering angles θ = 30, 50, 70, 90, 110, 130°.

The characteristic relaxation times τ_{VV} and τ_{VH} are such that: $1/\tau_{VV} = D\,q^2$ and $1/\tau_{VH} = D\,q^2 + 6D_{rot}$. The slope of $1/\tau_{VV}$ versus q^2 leads to $D=1.88\ 10^{-12}$ m^2/s. Extrapolating $1/\tau_{VV}$ to $q^2= 0$ leads to $D_{rot}= 10.4$ s^{-1} (see Figure 8).

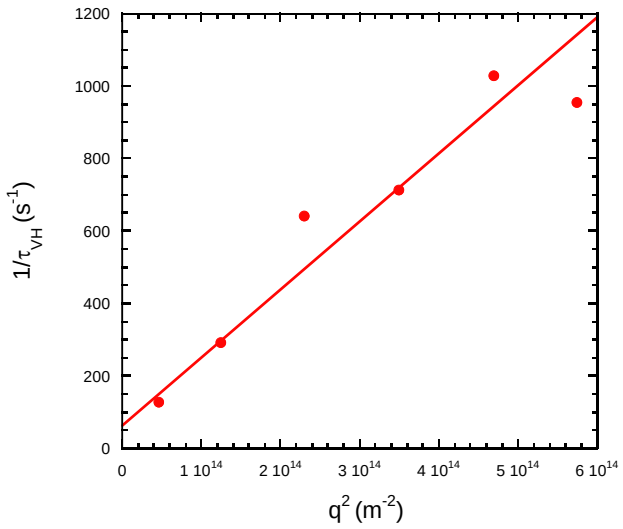

Figure 8. Variation of $1/\tau_{VH}$ with q^2. The line is the fit with $1/\tau_{VH} = D\,q^2 + 6D_{rot}$ using the diffusion coefficient determined from τ_{VV}.

Knowing D and D_{rot}, one can calculate the length L and the radius r of the nanotube following equation 9. One finds: r = 1.8 ± 1 nm and L ~ 1.3 μm. The PDI is large**,** around 0.6, likely because of the polydispersity in length of the nanotubes. AFM or SEM images of similar nanotubes gave L values between 500 and 1500 nm (14), in good agreement with the value measured here. The determination of r is the less precise, because it appears in a logarithm in equations 9. The mean r value is slightly larger than that measured with AFM: r = 1 ± 0.2 nm (13), but the agreement is reasonable in view of the error bars.

In the special cases of gold nanorods and gold-platinum Janus nanoparticles it has been observed that polarized light scattering alone is able to detect two modes attributed to the $D\,q^2$ and $D\,q^2 + 6D_{rot}$ (15; 16):

$$g_{1,VV}(\tau) = A_1 \exp(-Dq^2\tau) + A_2 \exp(-(Dq^2 + 6D_{rot})\tau),$$

where A_1 and A_2 are the amplitude of the modes.

It is interesting to notice that standard nanosizers are able to distinguish well the two modes given the backscattering geometry and the relatively high value of the scattering vector ($\theta = 173°$) (15).

These methods can of course be applied to other types of anisotropic particles. Relations between R_g and R_h or R_h and D_{rot} have been established for other type of particles. In the case of particular shapes, they can be computed on purpose (17).

In the general case, and even for spherical particles, it is quite useful to perform measurements at different q and concentrations; extrapolations to zero allow measuring more accurately the diffusion coefficients and they can also provide additional information as the interparticle interactions (using equation 4)

6. Conclusion

Dynamic light scattering is a very versatile method for the study of Brownian motion of nanoparticles in a liquid medium. Although its main application is for particles sizing, it is not the more accurate method for polydisperse samples. Indeed, particles of larger sizes scatter light more efficiently, hence the scattering is dominated by the fraction of particles of larger size. The average size is therefore shifted with respect to the size measured by electron microscopy for instance. The results provided by commercial instruments should be considered as indicative, especially those obtained with inversion methods. Significant errors could be made when working with dilute dispersions of very small particles that scatter little light. When the instruments allow retrieving the correlation function data, the results can be analyzed in more detail, taking into account the actual noise of the correlation functions, and better estimations of the sizes can be made.

One of the great interest of the DLS technique is the possibility to obtain additional information, for instance on hydrodynamic interactions between particles when their concentration is sufficient (volume fractions above a few percent). Anisotropic particles cause depolarization of the scattered light and when using polarizers, information about shape can be obtained.

In the case of particles of arbitrary shapes, it is difficult to assess their precise shape using light scattering only, and a combination of the technique with electron microscopy for instance is recommended. When the polydispersity is very high, the method is not recommended either, other methods are to be preferred (18).

Acknowledgements

The work presented here has been supported by the EU FP7 Capacities project QualityNano (grant no. INFRA-2010-262163). We also would like to acknowledge Robert Jack (Malvern Instruments) for helpful discussions.

References

1. Kerker M. 1969. *The Scattering of Light and Other Electromagnetic Radiation*. Academic Press. v pp.
2. Berne BJ, Pecora R. 2000. *Dynamic light scattering: with applications to chemistry, biology, and physics*. Courier Corporation
3. Russo P. 2012. *http://macro.lsu.edu/howto/DLS_Minicourse/DLS_Minicourse.pdf*.
4. Russel WB. 1981. Brownian-motion of small particles suspended in liquids. *Annu. Rev. Fluid Mech.* 13:425-55
5. Ostrowsky N, Sornette D, Parker P, Pike ER. 1981. Exponential sampling method for light-scattering polydispersity analysis. *Optica Acta* 28:1059-70
6. authors. in preparation. Interlaboratory comparison of size measurements on nanoparticles using dynamic light scattering (DLS) and differential centrifugal sedimentation (DCS).
7. de Frutos M, Letellier L, Raspaud E. 2005. DNA ejection from bacteriophage T5: Analysis of the kinetics and energetics. *Biophysical Journal* 88:1364-70
8. Lozano O, Laloy J, Alpan L, Mejia J, Rolin S, et al. 2012. Effects of SiC nanoparticles orally administered in a rat model: Biodistribution, toxicity and elemental composition changes in feces and organs. *Toxicology and Applied Pharmacology* 264:232-45
9. Mejia J, Piret JP, Noel F, Masereel B, Toussaint O, Lucas S. 2013. Dose assessment of SiC nanoparticle dispersions during in vitro assays. *Journal of Nanoparticle Research* 15
10. Doi M, Edwards SF. 1986. *The Theory of Polymer Dynamics*. New York: Oxford University¨Press
11. Brenner H. 1974. Rheology of a dilute suspension of axisymmetric Brownian particles. *International Journal of Multiphase Flow* 1:195-341
12. Shetty AM, Wilkins GMH, Nanda J, Solomon MJ. 2009. Multiangle Depolarized Dynamic Light Scattering of Short Functionalized Single-Walled Carbon Nanotubes. *Journal of Physical Chemistry C* 113:7129-33
13. Knyazev A, Louise L, Veber M, Langevin D, Filoramo A, et al. 2011. Selective Adsorption of Proteins on Single-Wall Carbon Nanotubes by Using a Protective Surfactant. *Chemistry-a European Journal* 17:14663-71
14. Campidelli S, Ballesteros B, Filoramo A, Diaz Diaz D, de la Torre G, et al. 2008. Facile decoration of functionalized single-wall carbon nanotubes with phthalocyanines via "Click Chemistry". *Journal of the American Chemical Society* 130:11503-9
15. Glidden M, Muschol M. 2012. Characterizing Gold Nanorods in Solution Using Depolarized Dynamic Light Scattering. *Journal of Physical Chemistry C* 116:8128-37
16. Lee TC, Alarcon-Correa M, Miksch C, Hahn K, Gibbs JG, Fischer P. 2014. Self-Propelling Nanomotors in the Presence of Strong Brownian Forces. *Nano Letters* 14:2407-12
17. Feitosa K, Durian DJ. 2008. Gas and liquid transport in steady-state aqueous foam. *Eur. Phys. J. E* 26:309-16
18. Schuler B, Meyer G, Peña D, Mullins OC, Gross L. 2015. Unraveling the Molecular Structures of Asphaltenes by Atomic Force Microscopy. *Journal of the American Chemical Society* 137:9870-6